Bulletin of the Seismological Society of America, 89, 2, pp. 521–537, April 1999

# Site Effects in the City of Thessaloniki (Greece) Estimated from Acceleration Data and 1D Local Soil Profiles

by Petros Triantafyllidis, Panagiotis M. Hatzidimitriou, Nikos Theodulidis, Peter Suhadolc, Costas Papazachos, Dimitris Raptakis, and Kostas Lontzetidis

Abstract In this study, the site effects on seismic ground motion in the city of Thessaloniki (Greece) are estimated by applying experimental methods on acceleration data and theoretical modeling. The technique of standard spectral ratio (SSR) is applied to a reference station located on rock, while the horizontal-to-vertical spectral ratio (HVSR) technique is applied to earthquake records (entire record length including *P* and *S* waves) as well as on noise recordings. In addition, the SSR method is also applied to the vertical components. The results from all methods are compared in terms of resonant frequencies and amplification levels. The fundamental resonant frequency is identified by all methods, while the average amplification level is generally underestimated when the HVSR technique is used. An attempt is made to correlate the site amplifications computed in this study with the observed macroseismic intensities reported at the same sites for the 20 June 1978 earthquake. A relation of the form, $\delta I = \alpha + b \cdot \log[\overline{SSR}(f)]$ is derived, where $\delta I$ is the intensity increment with respect to the intensity of the reference station and $\overline{SSR}(f)$ is the mean amplification factor obtained at each station using the SSR technique for a certain frequency band. In the numerical approach, we construct complete strong-motion synthetics using the modal summation method for the *P-SV* waves up to frequencies of 10 Hz. As input, four point sources are used, located at different distances and azimuths from the stations. Ratios of response spectra of the local 1D over the regional 1D synthetic seismograms are calculated. The obtained mean spectral amplifications are compared with those derived from experimental data, and the two sets are found to be consistent at most stations.

## Introduction

After the occurrence of large destructive earthquakes during the last 10 years, such as the Mexico 1985 (e.g., Bard and Chávez-García, 1993), the Armenia 1988 (e.g., Borcherdt *et al.*, 1989), the Loma Prieta 1989 (e.g., Hough *et al.*, 1990), the Northridge 1994 (e.g., EERI, 1994), and the Kobe 1995 (e.g., EERI, 1995), both seismologists and earthquake engineers have focused their attention on the importance of local site response on seismic ground motion. The observed unequal distribution of damage from these earthquakes promoted a series of studies on scenarios and parameters concerning local geological conditions responsible for the differentiation of the seismic ground motion. Indeed, many factors affect the seismic motion near the recording site: seismic-wave velocities and geometry of the stratigraphy (the thickness and position of the discontinuities of the geological formations), topography (Boore, 1972, 1973; Bard, 1992), and intensity of excitation (weak or strong) that can induce nonlinear phenomena in correlation with local geology (Aki, 1993; Field *et al.*, 1997). Generally, the big variety of classifications of site effects confirms the complexity and the still inadequate understanding of the physics of this phenomenon (Aki, 1988, 1993; Bard, 1995; Kudo, 1995). Without pretending to properly define such a complex phenomenon, we can very roughly summarize that both near-surface heterogeneities and topography are responsible for the observed different features of the wave field, causing amplification (or deamplification) of the seismic motion at the surface. The quantitative estimation of this phenomenon is usually given in terms of the level of the site amplification for the relevant frequency band.

One of the first attempts to estimate site effect was done by Lawson *et al.* (1908) after the 1906 earthquake of San Francisco. In the first investigations, macroseismic observations were used, but later on, data from instrumental recordings became the predominant tool for the estimation of site effects. In the last years, a multitude of experimental methods for site-effect estimation have been proposed, as well as improvement of existing or development of new nu-

merical techniques for estimating the response of superficial layers (e.g., Borcherdt, 1970; Nakamura, 1989; Fäh, 1992; Lermo and Chávez-García, 1993; Field and Jacob, 1995).

In this article, we deal with site-effect estimates in the city of Thessaloniki (northern Greece), which is located close to a major seismogenic area and had experienced several destructive earthquakes during the present century (Papazachos and Papazachou, 1997). The last earthquake sequence occurred during May through July 1978, with three earthquakes of $M_S$ magnitudes 5.8, 6.5, and 5.1 at a distance of about 30 km NE from the city (Papazachos *et al.*, 1979; Carver and Bollinger, 1981; Soufleris *et al.*, 1982). These events were the first large earthquakes that hit a modern greek city and had important economic and other social consequences. In the city, an apartment house collapsed and thousands of buildings suffered nonrepairable damage (Papazachos and Papazachou, 1997). Due to its interesting position and previous experience, some studies have already been conducted in the area of Thessaloniki to assess the geophysical and geotechnical characteristics responsible for site effects in this city (Chávez-García *et al.*, 1990; Raptakis *et al.*, 1993; Raptakis *et al.*, 1994b; Anastasiadis, 1994; Raptakis, 1995; Lachet *et al.*, 1996). We also compare the estimates of site effects as derived from macroseismic and instrumental data for selected sites in the city of Thessaloniki to those estimated theoretically from local 1D models.

## Data

The seismological data used in this study were acquired in the framework of a joint project among the Geophysical Laboratory of Aristotle University of Thessaloniki, the Institute of Engineering Seismology and Earthquake Engineering (ITSAK) of Thessaloniki, and the Laboratoire de Geophysique Interne et Tectonophysique (IRIGM-LGIT), University of Joseph Fourier, Grenoble.

The experiment was carried out between November 1993 and February 1994. During this period, a portable network of seismometers and accelerometers was deployed in selected sites within the city of Thessaloniki. At each site, a six-component RefTek station was installed, equipped with a three-component accelerometer (Guralp CMG5). Eight stations also had a broadband three-component velocimeter (Guralp CMG40, $T_0 = 20$ sec), while 3 stations had a short-period ($T_0 = 0.5$ sec) Mark Product L22 sensor. In this study, only the data recorded by the deployed accelerometers are used. The positions of the 11 stations of the temporary network as well as the sensor type used at each site are shown in Figure 1. The selection of the sites was based on the observed macroseismic intensities due to the Thessaloniki ($M_S = 6.5$) earthquake of 20 June 1978 with the aim to correlate the transfer function at each site with the locally observed intensity increments. At all sites, geotechnical testings and an extended geophysical survey (cross-hole, down-hole, surface-wave inversion) have been carried out by the Laboratory of Soil Mechanics & Foundation Engineering of

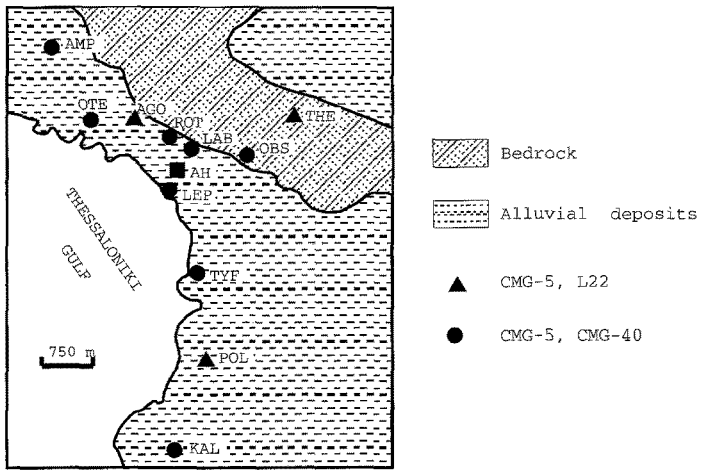


Figure 1. Location of the temporary seismological stations on the map of Thessaloniki and type of sensor used at each site. The square at AH shows the site of the apartment house that collapsed after the June 1978 earthquake [modified after Raptakis (1995)].

Aristotle University of Thessaloniki (Anastasiadis, 1994; Raptakis, 1995). At each site, the obtained geometry and dynamic soil properties (body-wave velocities, quality factors) have been used for the theoretical estimation of the local seismic motion amplification.

Stations OBS and THE (Fig. 1) were placed on hard rock (gneiss) as reference stations. All other stations were installed on various formations (sedimentary deposits) covering the different geological conditions of the city. In our analysis, we will, however, not consider the recordings obtained at station LEP, because the noise level at this site was very high, producing a poor signal-to-noise ratio. Because all the stations were located within the city, where the ground noise is very high, each RefTek was connected telemetrically with the Seismological Observatory of Thessaloniki, where a radio system was set up to reject false triggerings.

During the period of network operation, more than 100 events have been recorded. From these, we have selected only those that had also been well recorded by the Seismological Observatory. This selection produced a catalog of 34 earthquakes, whose epicenters are plotted in Figure 2. The $M_L$ magnitude range of these earthquakes varies from 1.4 to 4.2, and the range of hypocentral distances varies from 5 to 154 km. The locations of the earthquakes are given in the monthly bulletins of earthquakes of the Geophysical Laboratory of Aristotle University of Thessaloniki.

After the baseline correction and removal of spikes, glitches, etc., two windows have been selected containing, respectively, noise and signal ($P$ and $S$ waves). Almost in all cases, the window of noise has been selected before the $P$-wave arrival and had a duration from 5 to 20 sec. In a few cases, either because of electronic noise or because of a high ambient noise level before the $P$-wave arrival that was ob-

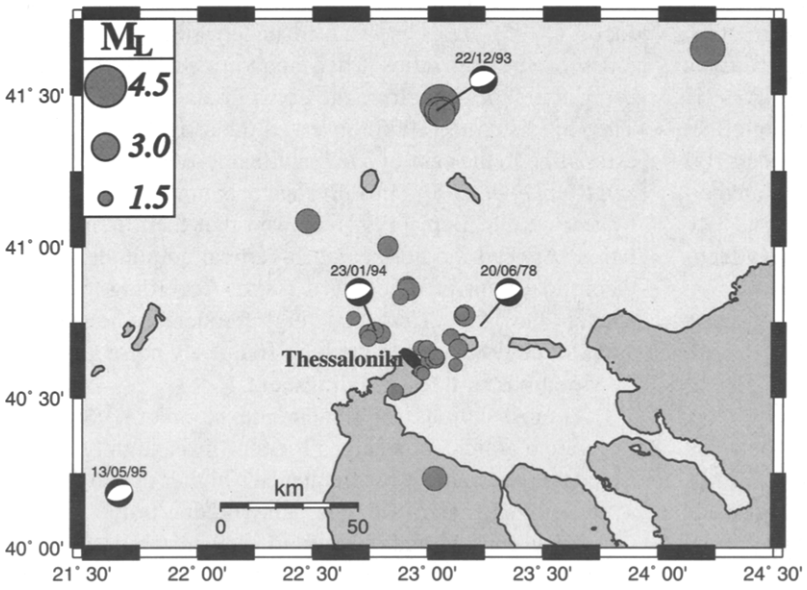


Figure 2. Location of the epicenters of the earthquakes recorded by the portable network and the focal mechanisms of the four events used as input for the construction of the synthetics.

viously not included in the signal, the noise window has been taken after the end of the signal.

When computing spectral ratios, we have used as a signal the entire record length (including *P* and *S* waves). There are two main reasons for using the entire record length instead of separating the high-amplitude *S*-wave part of the motion. First, in structural response evaluations for seismic excitation, the entire accelerogram is usually used; second, the separation of a particular type of wave from the record is not a straightforward task because of scattering effects that affect all parts of the signal except the very onset of *P* waves.

We used, in total, almost 360 records of horizontal and 120 of vertical components of noise and the same for signal, treating the horizontal components independently. An FFT algorithm has been applied to the part of the waveform selected as signal to calculate spectral amplitudes. The sampling interval in time domain was $\Delta t = 0.008$ sec. The obtained spectra have been smoothed with a running average frequency window of 0.5 Hz with 50% overlap. The signal-to-noise spectral ratio was calculated for all the waveforms, and the recordings with values greater than 1 were considered for further analysis.

## Experimental Methods

One of the methods for the estimation of site amplification used in this study is the reference station technique called standard spectral ratio (SSR). In this technique, first introduced by Borcherdt (1970) and still widely used, the horizontal records at each site are compared with the horizontal records for the same events at a nearby bedrock site (reference site) through spectral ratios. The ratio of the amplitude spectrum of a record at a given site over the amplitude spectrum of the record at the reference site is considered to be a measure of the site effect on ground motion in the case that the following two assumptions are valid (Borcherdt, 1970; Steidl *et al.*, 1996): (1) the reference station is free or almost free from local amplification effects and can be used at least for relative estimates of the local amplification, and (2) the distance between the source and the two receivers is much greater than the distance between the receivers themselves. According to these assumptions, the differences in the records at the two sites are only due to local site conditions and not to differences in the source radiation or wave propagation.

For the application of this method, station OBS is used as a reference station because it is located on bedrock (Fig. 1), and it is slightly closer to the other stations than the bedrock station THE. According to several surveys (Singh *et al.*, 1988; Campillo *et al.*, 1989; Chávez-García, 1991), it is suggested that the vertical component of ground motion is not affected by site effects as much as the horizontal components and may be thus used to measure the incident ground motion, that is, the motion not yet affected by local site conditions. However, Riepl *et al.* (1998) showed that the vertical component can be strongly affected by local amplification effects, if the geology is complex. In order to check this assumption in the rather complex geology of Thessaloniki, the SSR method using the same reference station is applied also to the vertical components.

Another commonly applied method for site effect estimates is the horizontal-to-vertical spectral ratio (HVSR) method (i.e., ratio between the smoothed Fourier spectra of the horizontal and vertical components). This technique was initially introduced by Nogoshi and Igarashi (1970, 1971) in Japanese, who applied it to microtremor measurements. This method is in fact a combination between a seismological method [called the receiver function (RF) technique] used by Langston (1979) to determine the velocity structure of the crust from the HVSR of teleseismic *P* waves and the

proposal of Nakamura (1989) to use this ratio on ambient noise recordings. When applying the HVSR method to noise data, it is assumed that the microtremor energy consists mainly of Rayleigh waves (Nogoshi and Igarashi, 1971; Lachet and Bard, 1994; Kudo, 1995) and that the site-effect amplification is due to the presence of a soft surficial soil layer overlying a half-space. In this study, the HVSR method is applied both to the whole (*P* and *S* waves) signal (RF technique) and to the noise portions of the records (HV technique).

## Discussion of Results Obtained by Experimental Methods

Figure 3 presents the variation with frequency (between 0.5 and 20 Hz) of the mean local site amplification, as obtained by the application of the three spectral ratio methods (SSR, RF, and HV) to each site. Examining the shape of the SSR amplification (solid line), it can be realized that besides the stations located on bedrock (OBS, THE), also the stations POL and KAL have a very low amplification level (between 1 and 2) in the whole frequency range. Stations AMP, OTE, and TYF, on the other hand, present a significant amplification level with maximum values between 3 and 5 at frequencies between 4 and 8 Hz. TYF presents a constant amplification level even in the low-frequency (0.5 to 5 Hz) range. Both stations ROT and LAB have an amplification level between 2 and 3 up to 9 Hz, whereas for higher frequencies, levels are higher. LAB reaches a maximum amplification (around 6.5) in the frequency range between 9 and 12 Hz, while the highest amplification (around 10) of ROT is obtained at frequencies in the range 18 to 20 Hz. Finally, AGO has strong amplifications between 4 and 12 Hz, with a peak around 10 Hz.

Regarding the HVSR results, both RF (dashed line) and HV (dotted line) techniques, spectral shapes are generally in good agreement with each other (with the exception of KAL and POL), and the frequency band in which the maximum amplification appears for both techniques is consistent with the one from the SSR at each site. However, at ROT and AGO, we do not observe the high amplification levels at frequencies higher than 12 Hz as in the case of the SSR method. This means that the vertical component at these stations has been influenced by site effects in this frequency range. Lachet *et al.* (1996) got a similar result and explained it as being due to archeological ruins that are present at shallow depths at these two sites.

It is not easy to identify the fundamental frequency of the soil amplification at all stations, but when this is possible (e.g., 2 Hz at OTE, 3 Hz at LAB, and 7 Hz at AGO), we notice that all methods generally agree in determining it. We also observe an agreement in the spectral shape for the different ratios at each site, at least for frequencies up to 5 to 6 Hz. For greater values of frequency, the amplitudes obtained by HVSR techniques are generally underestimated in comparison with the amplitudes of SSR. This is particularly evident at stations AMP, OTE, ROT, and AGO. Field and Jacob (1995) also observed an underestimation of amplitudes of spectral ratios when applying the HVSR method using aftershock data from the Loma Prieta 1989 earthquake. Theodulidis *et al.* (1996) observed the same kind of underestimation in the case of site amplifications in Garner Valley and Riepl *et al.* (1998) in Volvi basin. Numerical simulations by Lachet and Bard (1994) showed that there is no correlation between the horizontal-to-vertical amplitude and the theoretical transfer function of a site. According to Lachet *et al.* (1996), the difference at high frequencies between RF and SSR could be due to the high-frequency noise generated by vibrations of trees, buildings, etc.

At most stations, the standard deviation of HVSR methods varies around 2, whereas for SSR, it is slightly higher, exceeding the value 3 for frequencies higher than 6 Hz only at stations KAL and POL. This may be due to the constant frequency content and wave-field type in the case of (repeatable) noise, whereas the wave-field characteristics of individual earthquakes can vary greatly (Lachet *et al.*, 1996; Riepl, 1997). Significant variations in the SSR for different earthquakes at the same site have also been obtained by Lermo and Chávez-García (1994). Some possible effects of anisotropic radiation and propagation path differences may exist in the standard deviation of SSR estimates. Figure 4 shows two sites where the lower (AGO) and the higher (KAL) values of standard deviation are observed.

In Figure 5, a comparison is made between the arithmetically averaged amplification for different frequency bands as estimated at each site by the SSR method applied to vertical component (VSSR), RF, and HV (left to right, respectively) and the corresponding average amplification as estimated from SSR. At each site, the mean amplification was calculated for specific frequency ranges (0.5 to 1 Hz, 1 to 2 Hz, and then every 2 Hz up to 18 Hz), and the results were grouped together for frequency bands that are written on top of each plot of Figure 5. It can be clearly seen from that figure that the HV and RF methods underestimate the amplification amplitudes especially for frequencies higher than 6 Hz, whereas the scatter of the data increases with frequency. Furthermore, it seems that there is a very good correlation up to 6 Hz between SSR applied to horizontal and vertical components. The amplification that is observed on vertical component is significant at all stations, particularly at high frequencies, which agrees with the results of Riepl *et al.* (1998).

All the foregoing results are generally in good agreement as it was expected with the results obtained by Lachet *et al.* (1996), who used velocity data at the same sites. The main characteristics at each site are very similar either using velocity data or acceleration data. At stations POL, THE, and AGO, the previous authors used L22 sensors (Fig. 1), and therefore, their results are probably less reliable for frequencies below 2 Hz, due to the relatively poor response of this sensor in this frequency range. Also at stations KAL, AMP, and TYF, there is a disagreement in SSR estimates at fre-

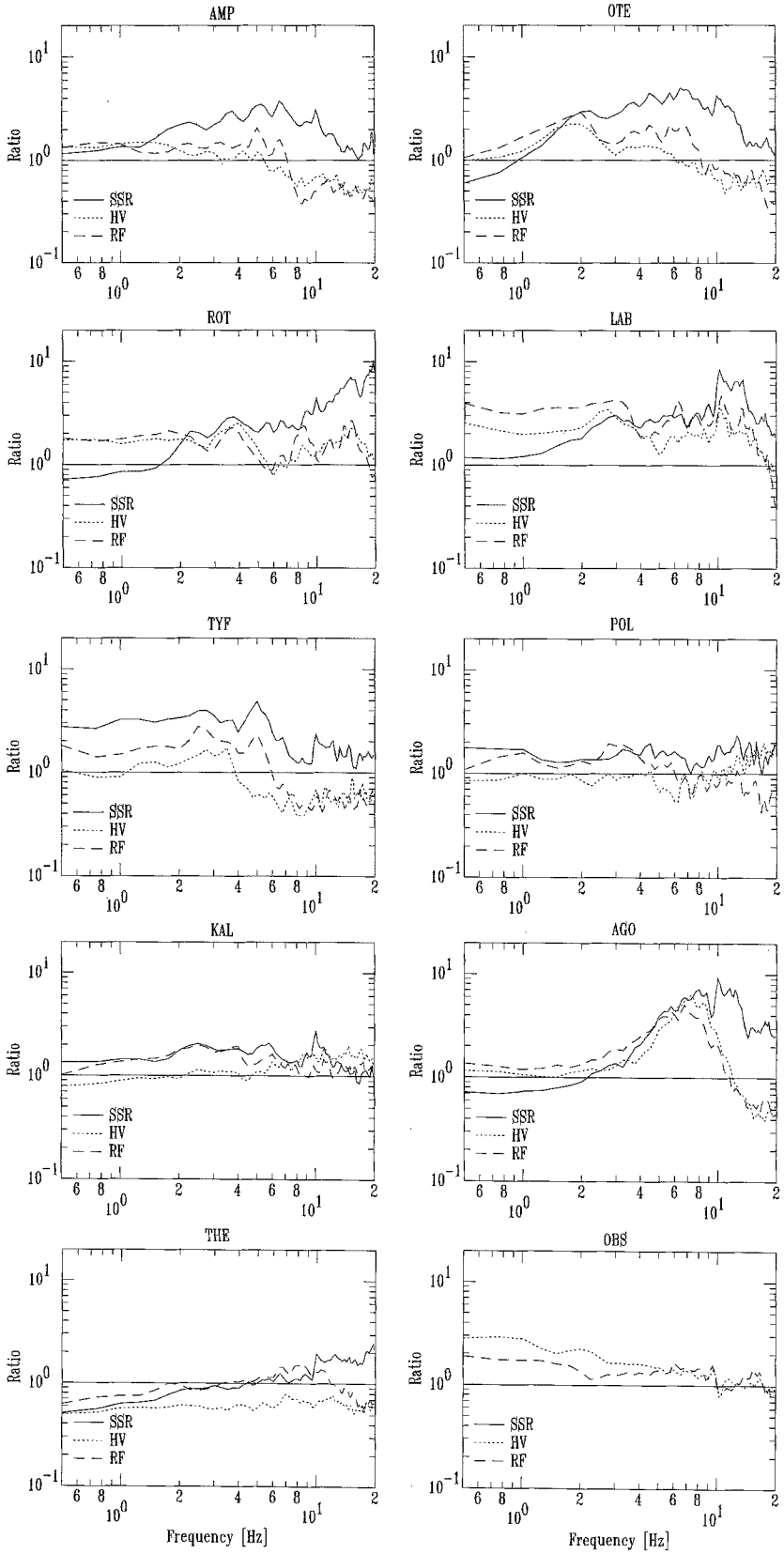


Figure 3. Variation with frequency of the mean local site amplification, as obtained by the application of the three spectral ratio methods. Solid line stands for Standard Spectral Ratio (SSR), dotted line for horizontal-to-vertical ratio for noise (HV), and dashed line for receiver function (RF).

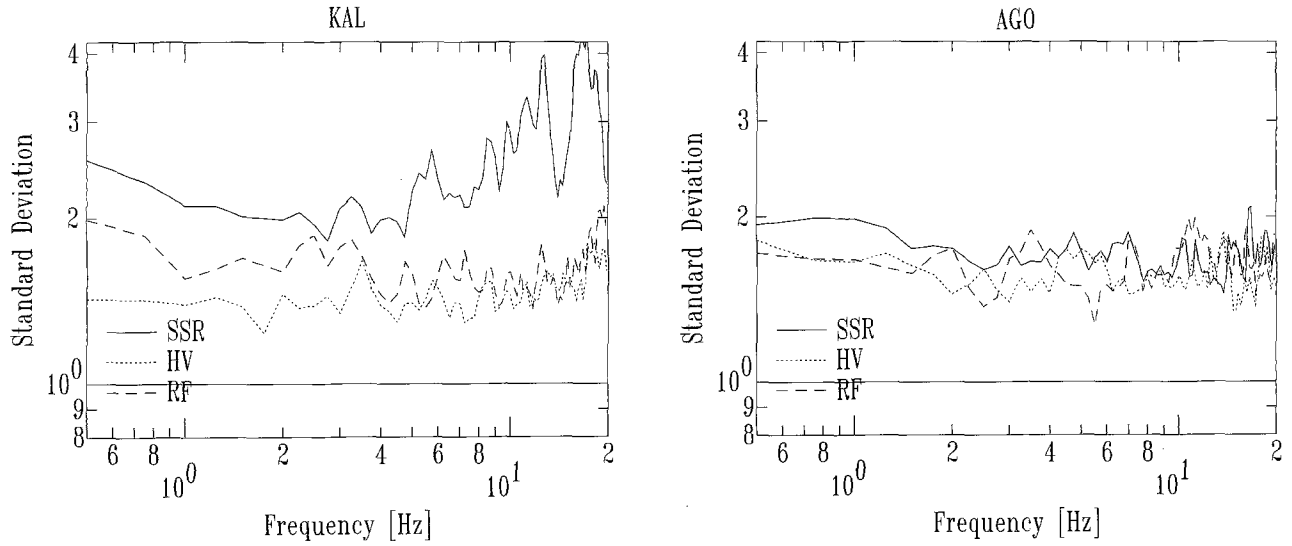


Figure 4. Variation of standard deviation with frequency for each method at sites KAL and AGO. The solid, dotted, and dashed lines represent the standard deviation of SSR, HV, and RF, respectively.

quencies below 2 Hz. This might be due to the differences between the sensors and the type of motion recorded.

## Correlation with Macroseismic Intensities

An attempt is made to correlate the estimated ground-motion amplifications at each site of the present study with the reported macroseismic intensities observed in the city of Thessaloniki during the 20 June 1978 earthquake. The main-shock was followed by a long sequence of aftershocks, and the largest of them ($M$ = 5.1) occurred on 4 July at 22:23:28.

Borcherdt and Gibbs (1976) used, for the city of San Francisco, data from nuclear explosions and computed the correlation between average horizontal spectral amplifications and intensity increments $\delta I$. The quantity $\delta I$ was estimated from the difference between the observed intensity from the 1906 San Francisco earthquake and the predicted one by an empirical relation of seismic intensity ($I$) versus the perpendicular distance from the zone of surface faulting for frequencies 0.25 to 3 Hz. As reference stations, they used various sites located on four different geological units: stiff clay and conglomerate, sandstone, greenstone over shale, and granite.

In this study, we modified the method of Borcherdt (1970) simply by correlating the logarithm of the mean amplification, for different frequency bands, with the observed intensity increment $\delta I$. The quantity $\delta I$ is the difference between the averaged intensity $I_i$ reported for the 1978 earthquake at a specific site (G. Leventakis, personal comm., 1998) and the reference intensity $I_R$ reported at the reference site (OBS). The empirical relations obtained with the least-squares method are of the form

$$\delta I = \alpha + b \cdot \log[\overline{SSR}(f)], \quad (1)$$

where $\overline{SSR}(f)$ is the mean amplification estimated with the SSR method for various frequency ranges $[f_{\min}, f_{\max}]$. The estimated parameters $\alpha$ and $b$ and the corresponding correlation coefficients $R$ for each frequency band are given in Table 1. The best correlation ($R$ = 0.91) has been obtained when considering the frequency range 3 to 6 Hz (Fig. 6a). On the same plot, the relation of Borcherdt and Gibbs (1976) for San Francisco, $\delta I = 0.27 + 2.70 \cdot \log[\overline{SSR}(f)]$, is shown by the thin dashed line. We have tried also to correlate in an analogous empirical way the intensity increments $\delta I$ with the logarithm of the RF for various frequency bands. The results, however, are not so encouraging as for the case of the correlation with the logarithm of SSR.

Taking into account the results of Borcherdt and Gibbs (1976), we made an attempt to check the validity of the suggested empirical relation (1) in the case of strong-motion data, represented by the recordings of the $M$ = 5.1 aftershock of the 1978 earthquake. The aftershock was recorded by several accelerographs, among others at site AH (Fig. 1) where an eight-story building collapsed and at the bedrock site OBS. Figure 7 shows the recordings at these two sites, and we can clearly see the amplification due to site effects at AH.

If we plot on Figure 6a the experimental point related to the AH site [its $\overline{SSR}(f)$ value is derived from the spectra of the two records shown in Fig. 7] in the frequency range 3 to 6 Hz, we observe that it is not well estimated by the regression line. Since the resonant frequency of an eight-story building, like the collapsed one, is most probably between 1 and 2 Hz, it might be more appropriate to extend the frequency range to lower frequencies. If the range 1 to 10 Hz is selected (Fig. 6b), the AH site datum is still not well predicted, but for the frequency range 1 to 5 Hz, the

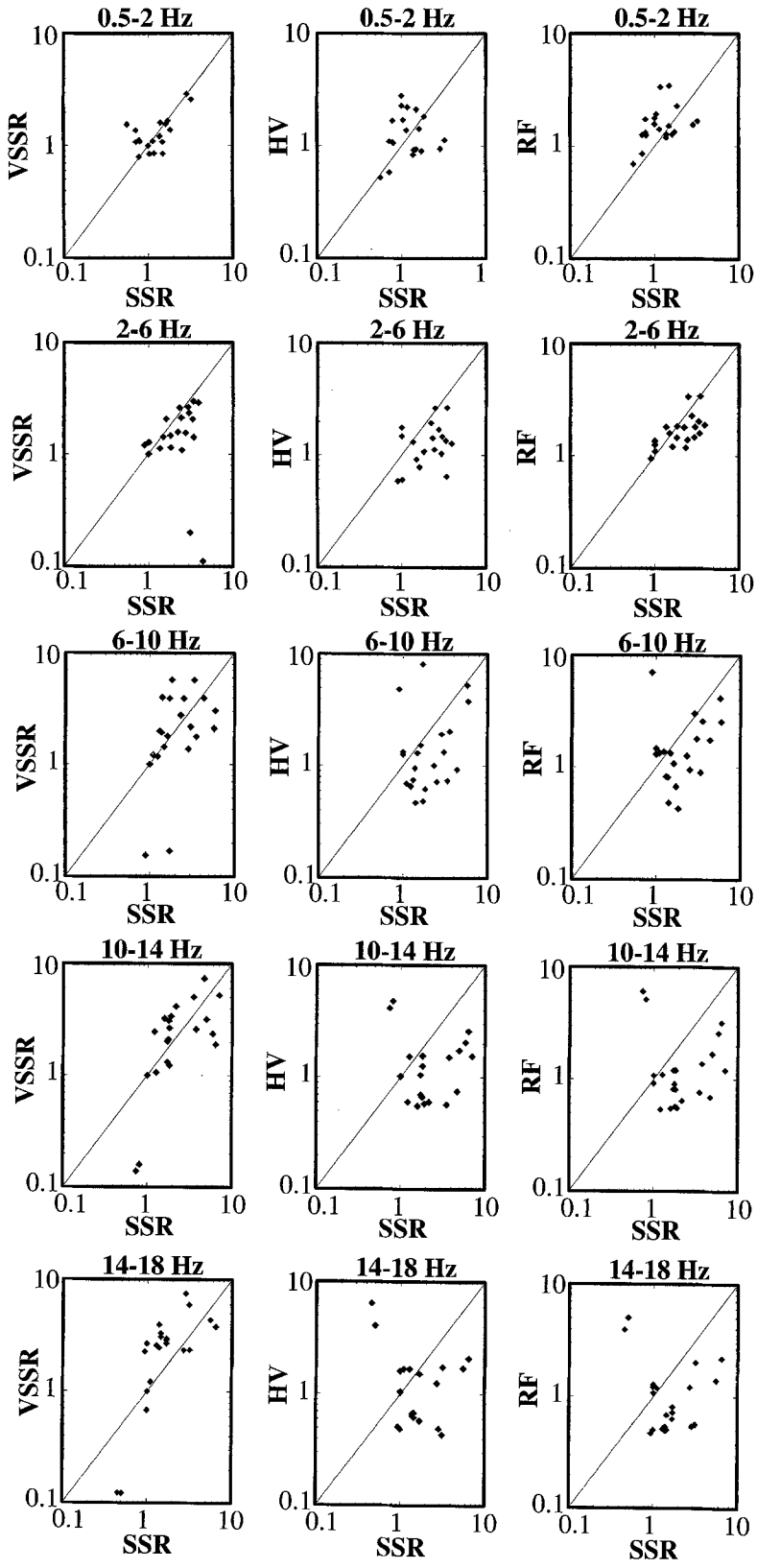


Figure 5. Comparison between the arithmetically averaged amplification at each site as estimated from the vertical-component SSR (VSSR) method, RF method, and HV method (left to right, respectively), and the arithmetically averaged amplifications at the same site as estimated from SSR for different frequency bands (top to bottom).

correlation line approximates much better the AH site datum (Fig. 6c).

It is obvious that in an *a priori* study, it would be difficult to choose the proper and reliable frequency range for which the $\overline{SSR}(f)$ should be estimated, taking also into account that all the sites do not amplify the motion in the same frequencies. Moreover, as it is evident from our regressions, the frequency range influences significantly the results. Therefore, we estimated the relation between $\log[\overline{SSR}(f)]$ and $\delta I$ for frequency range of 1-Hz width around the site fundamental frequency. The regression gave a relatively poor correlation coefficient ($R = 0.65$), and the AH site datum is not very well predicted. From all these regressions, it comes out that $\delta I$ is not only the result of differential ground motion relative to a bedrock site but a combination of local site amplification, the resonant frequency of the structure, the soil–structure interaction effects, and the vulnerability of the construction. It is difficult to deconvolve all these factors, and further research is needed on this subject. However, from the results presented here, it seems that the best fit between $\delta I$ and $\log[\overline{SSR}(f)]$ is achieved when we choose a frequency range wide enough to include both the resonant frequencies of the soil column at different sites and the resonant frequencies of the structures.

Chávez-García *et al.* (1990) also observed a good correlation between weak-motion data (recorded velocity from different events) near Thessaloniki and macroseismic information with that obtained by Borcherdt and Gibbs (1976). This good agreement shows an obvious linear behavior of the holocainic deposits at least up to an intensity VII (MM). We conclude that weak-motion data recorded in the city of Thessaloniki can be successfully used for the estimation of the future strong ground motion in the city. However, if we would like to estimate future damage of a construction, we have to rely on the regression curve based on the frequency band most appropriate for the resonant frequency of the investigated construction at each site.

## Theoretical Approach

For the theoretical 1D modeling, data from detailed geotechnical information derived from cross-hole measurements at each site were used (Pitilakis *et al.*, 1992; Raptakis *et al.*, 1994a; Raptakis, 1995). The initial values of body-wave velocities ($V_p$, $V_s$) and quality factors ($Q_p$, $Q_s$) have been averaged out with a depth increment of about 20 m. This simplification is made because the maximum frequency of computations, which is 10 Hz, corresponds to wavelengths generally greater than 20 m. Figure 8 shows the variation of density ($\rho$), *P*- and *S*-wave velocities ($V_p$, $V_s$), quality factors ($Q_p$, $Q_s$), and the $V_p/V_s$ ratio with depth for station ROT for the first 1 km of depth. For larger depths, each local site model is underlain by the regional velocity model that has been deduced from the work in the broader area of Serbomacedonian massif (where Thessaloniki belongs) done by Papazachos (1998) and Ligdas and Lees (1993). According to the regional model, $V_p$ and $V_s$ start increasing from 4850 m sec$^{-1}$ and 2800 m sec$^{-1}$, respectively, while $Q_p$ and $Q_s$ are 250 and 200, respectively. For the sites OBS and THE that are located on bedrock, their local site velocity model coincides with the regional model, whose velocity at 1 km depth is extended to the surface.

Table 1
Parameters of Relation (1) for Various Frequency Bands When the Amplification Is Estimated with SSR Technique

| $f_{min}$ | $f_{max}$ | $a$ | $b$ | $R$ |
|---|---|---|---|---|
| 0.25 Hz | 3 Hz | 0.83 | 2.35 | 0.62 |
| 1 Hz | 2 Hz | 0.92 | 2.07 | 0.56 |
| 1 Hz | 3 Hz | 0.70 | 2.48 | 0.70 |
| 1 Hz | 5 Hz | 0.41 | 2.98 | 0.83 |
| 1 Hz | 6 Hz | 0.29 | 3.21 | 0.87 |
| 1 Hz | 10 Hz | 0.20 | 3.40 | 0.85 |
| 2 Hz | 6 Hz | 0.18 | 3.16 | 0.90 |
| 3 Hz | 6 Hz | 0.13 | 3.12 | 0.91 |
| 5 Hz | 10 Hz | 0.61 | 1.89 | 0.62 |
| 6 Hz | 10 Hz | 0.73 | 1.60 | 0.55 |

$R$ represents the correlation coefficient.

The computations were performed for *P* and *SV* waves (Rayleigh modes); however, all of the computations presented here have a general validity and, with proper modifications, can be easily extended to the treatment of *SH* waves (Love modes). An algorithm based on the modal summation method (Panza, 1985; Panza and Suhadolc, 1987) was applied for the construction of complete strong-motion synthetics considering flat layering from source to each site, for a maximum frequency of 10 Hz.

The focal mechanisms in Figure 2 depict the epicenters of the four sources used as input for the construction of the synthetics. The local event in the east corresponds to the 1978 earthquake, and the focal mechanism used is the one proposed by Papazachos *et al.* (1979). The event in the SW corner of the map corresponds to the Kozani earthquake of 13 May 1995 ($M_S = 6.6$) (Hatzfeld *et al.*, 1997), whereas for the north and the close west events, the focal mechanism of the 1978 earthquake was used, which is in agreement with the general active stress field at the area of northern Greece (Papazachos and Kiratzi, 1996).

Figure 9 shows the radial and vertical component of synthetics obtained for the local and the regional velocity model at each station due to a point source located on the focus of the 20 June 1978 earthquake. The synthetic of station AMP had originally a very noiselike aspect as well as a very low amplitude level, because it happened to be in a minimum of the radiation pattern. In order to avoid treating an anomalous record that would give unreliable results, we have arbitrarily increased the azimuth of the source–receiver line by 10°, which amounts to moving the source by a few kilometers, while maintaining the epicentral distance.

For all four events, we have calculated for both the radial and the vertical component at the same station the ratios

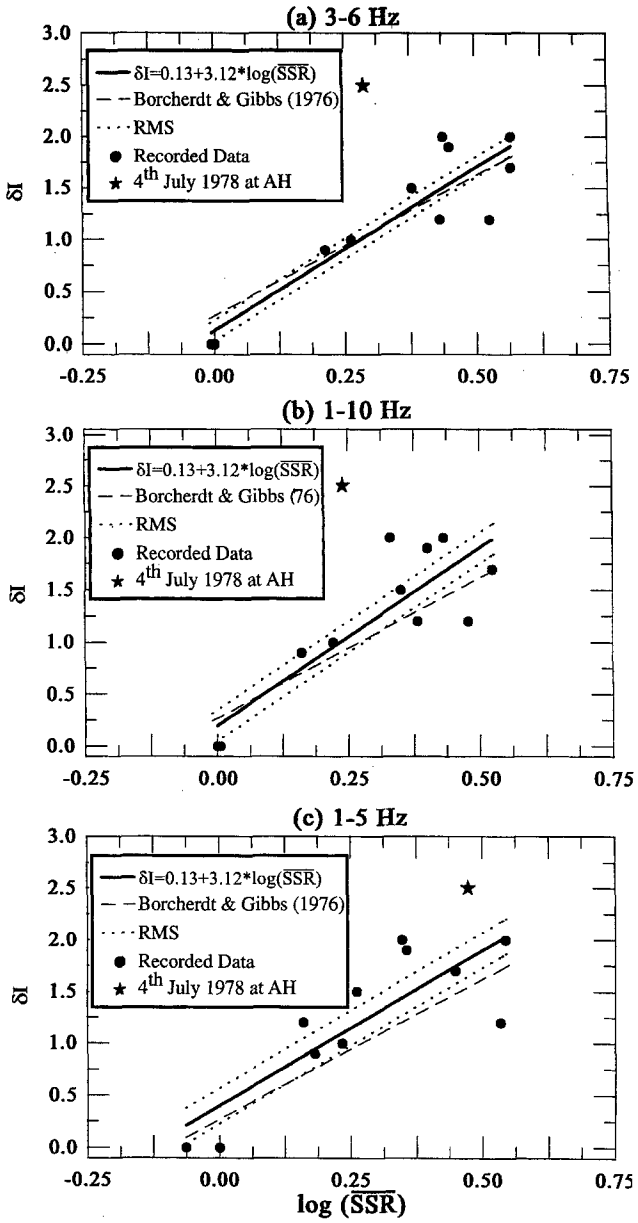


Figure 6. Correlation between the logarithm of the mean amplification (estimated with the SSR method) and the intensity increment $\delta I$ (thick solid lines), for different frequency bands: (a) 3 to 6 Hz, (b) 1 to 10 Hz, and (c) 1 to 5 Hz. The thin dashed line represents the relation of Borcherdt and Gibbs (1976) for San Francisco, $\delta I = 0.27 + 2.70 \cdot \log[\overline{SSR}(f)]$, while the dotted lines indicate the related rms error. The asterisk represents the average amplification at AH, the site of the collapsed building (see text).

of spectra of seismograms due to the local 1D velocity model over those due to the regional 1D velocity model. In order to check the validity of the reference station technique, we have computed also the spectral ratios of the local 1D seismograms to those of the reference station (OBS), both for radial and vertical components.

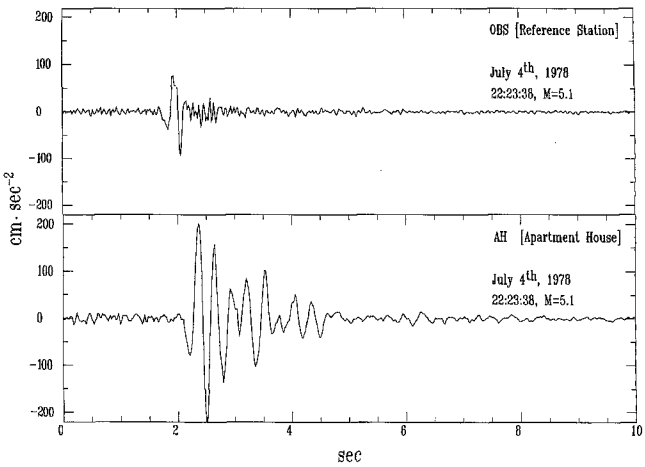


Figure 7. The acceleration records, horizontal components, of the largest aftershock of the Thessaloniki 1978 sequence occurred on 4 July ($M$ = 5.1), close to station OBS (*top*) and the site AH (Fig. 1) where the building collapsed (*bottom*).

The radial and vertical ratios at each site were almost similar in terms of spectral shape, although the amplitude level of local-to-reference station ratios was different, in particular for the close events. The reason for this is that the local-to-regional ratio for the 1D model is a division between computed spectra at the same station, while the local-to-reference station ratio for the 1D model is a division between spectra of seismograms at two different sites. The difference is mainly due to differences in distance as well as in azimuths between the seismograms, and the differences become quite significant, if the event is local and the source–receiver distance is comparable to the distance between the stations. In those cases when a reference station is in a minimum of radiation, the ratios will result in increased site-effect amplification.

In order to correct the local-to-reference station ratios of the local events for the source and radiation pattern effects, we have multiplied the spectra determined from a local 1D velocity model by a correction factor. This factor is simply taken as the ratio of reference station peak ground acceleration (PGA) over the station PGA for the regional model. With such a correction, the amplification curves are now only due to the local velocity model.

We have also observed for the two distant events quite high amplification levels at low frequencies up to around 3 Hz. On the contrary, for the two close events, low-amplification levels have been observed in this frequency range. This observation suggests that the amplification at low frequencies is better determined with far events, whose waves contain relatively low frequencies, while amplification in the high-frequency range is better constrained by recordings of local events. Figure 10 shows with dotted lines the local over regional 1D-model spectral ratios at each station for the radial components of the four events. The dotted lines in

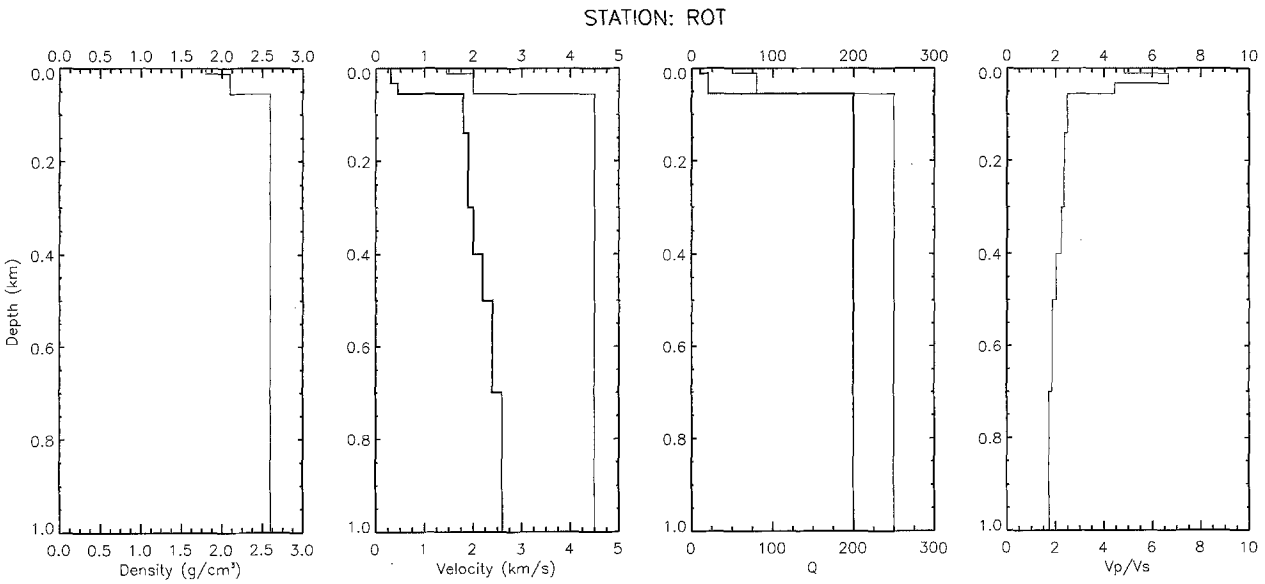


Figure 8. Variation of density ($\rho$), $P$-wave ($V_p$) and $S$-wave ($V_s$) velocities (thin and thick lines, respectively), quality factors ($Q_p$, $Q_s$; thin and thick lines, respectively), and the $V_p/V_s$ ratio with depth for station ROT (Raptakis *et al.*, 1994a; Raptakis, 1995).

Figure 11 show the variation of the local-to-reference station spectral ratios for the radial components of the far and the corrected close events. In both figures, the solid line represents the mean of all four ratios. The two types of ratios agree quite well in terms of both amplification level and spectral shape. There is also a satisfactory agreement in the frequencies where the amplification peaks appear.

Next we compare in Figure 12 the mean of spectral ratios of theoretical local-to-regional 1D model for the radial component with the mean of the SSR derived from the experimental data. In general, at all stations, both ratios are comparable, which means that our theoretical 1D estimates represent a rather good preliminary estimation of the expected amplification level. There are, of course, several discrepancies, especially at some stations.

In station AMP, a good agreement is observed only for frequencies up to 4 Hz, whereas for higher frequencies, the theoretical amplification underestimates the observed one almost by a factor of 2. A similar result can be seen also at station TYF, although only between 4 and 6 Hz. A good agreement, almost at all frequencies, is observed at stations LAB, POL, and KAL, where both experimental and theoretical amplification are approximately at the same level. At OTE, we observe the worst match between the two means. The experimental amplification is increasing almost continuously up to a factor of 5 at 7 Hz, while the theoretical amplification presents a maximum (a factor of 4) from 0.8 to 1.5 Hz and an almost stable level around 2 for higher frequencies. A similar behavior is noticed at station ROT, although the agreement is much better for frequencies higher than 2 Hz. At AGO, the experimental mean is lower than the theoretical one but only for frequencies up to 5 Hz. For higher values of frequency, the experimental data show an amplification almost two times higher than the theoretical ones. For station THE, the experimental results give a very low amplification, which is very close to the theoretical one, that equals 1. Finally, for station LEP, we have no qualitative experimental data, and no comparison is made.

Concluding, the general trend (Fig. 12) is that at low frequencies, from 0.5 up to 2 to 4 Hz, the theoretical amplifications are higher than the experimental. At higher frequencies, the opposite is generally observed. TYF is an exception because theoretical is lower for all the frequencies. LAB, POL, and KAL show good agreement in the whole frequency range, whereas ROT shows good agreement only at high frequencies. The differences noticed between the two types of means can be due to the fact that the theoretical one is the average of radial ratios of only four events and also to 2D and 3D effects in the wave propagation that are not taken into account in our 1D modeling.

## Conclusions

In the first part of this study, a comparison was made between the results of different experimental techniques for estimating site-effect amplification, using accelerometer data to an area characterized by relatively thick sedimentary deposits, but without large velocity contrast in the different formations. This explains the relatively low-frequency range in which the maximum amplification is observed at each site. The results obtained from the experimental approach are as follows:

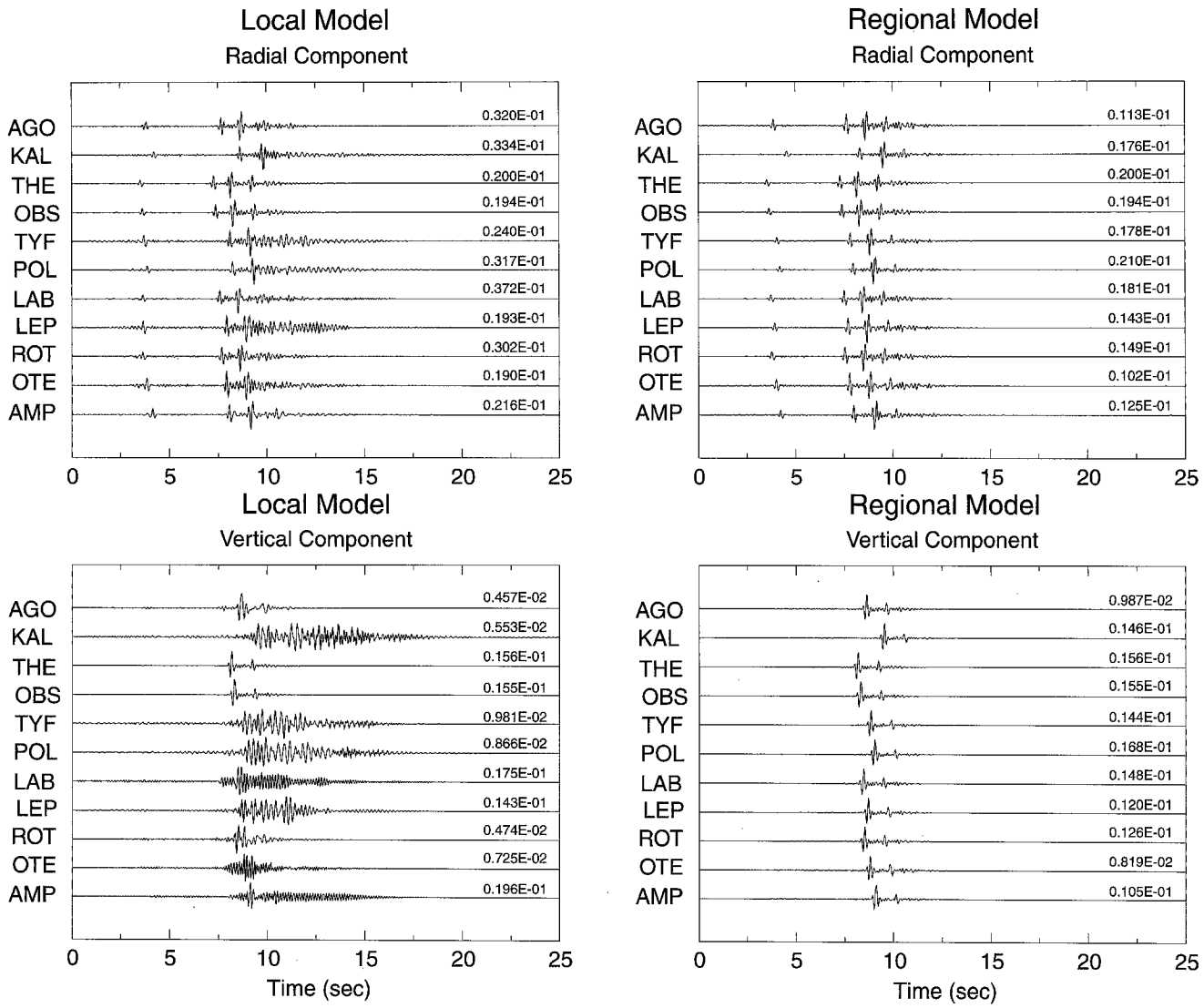


Figure 9. Radial (*top*) and vertical (*bottom*) component of synthetics obtained for the local (*left*) and the regional (*right*) velocity model at each station due to a point source located in the epicenter of the 20 June 1978 earthquake. In order to enhance the low-frequency part of the signal, we smoothly filtered the waveforms with a gaussian filter from 4 to 10 Hz.

1. Both SSR and HVSR (for signal or noise) techniques in the case of the rather complex geology of Thessaloniki give comparable amplification estimates for the frequency range that engineering seismology is mainly interested in, that is, up to 6 Hz. They also agree in identifying, when this is possible, the fundamental frequency and the frequency range in which the maximum amplification is observed. Finally, for frequencies higher than 8 Hz, the amplification derived from the SSR technique is systematically higher than that derived from HVSR. This observation is probably due to the selective enrichment of the vertical component of the scattered wave field. In other words, the incident wave field propagates mainly vertically close to the surface, and the greater part of energy reflected at the surface is trapped between the superficial layers (Finn and Nichols, 1988; Silva, 1989; Finn, 1991). The same interpretation, namely, the local site conditions effect due to 2D and 3D heterogeneities in the superficial layer, is given also for the case of Garner Valley (Theodulidis *et al.*, 1996) and for the case of Volvi basin (Riepl *et al.*, 1998; Raptakis *et al.*, 1998). In any case, as the aforementioned authors summarize, the differences in the amplitudes as derived from the various techniques is one problem that requires further study and investigation.
2. The HVSR techniques present a lower standard deviation than the SSR technique. This shows that the former ones are more stable than the latter one. This can be due mainly to the fact that by taking the horizontal-to-vertical spectral ratio, the source and travel path effects are eliminated.

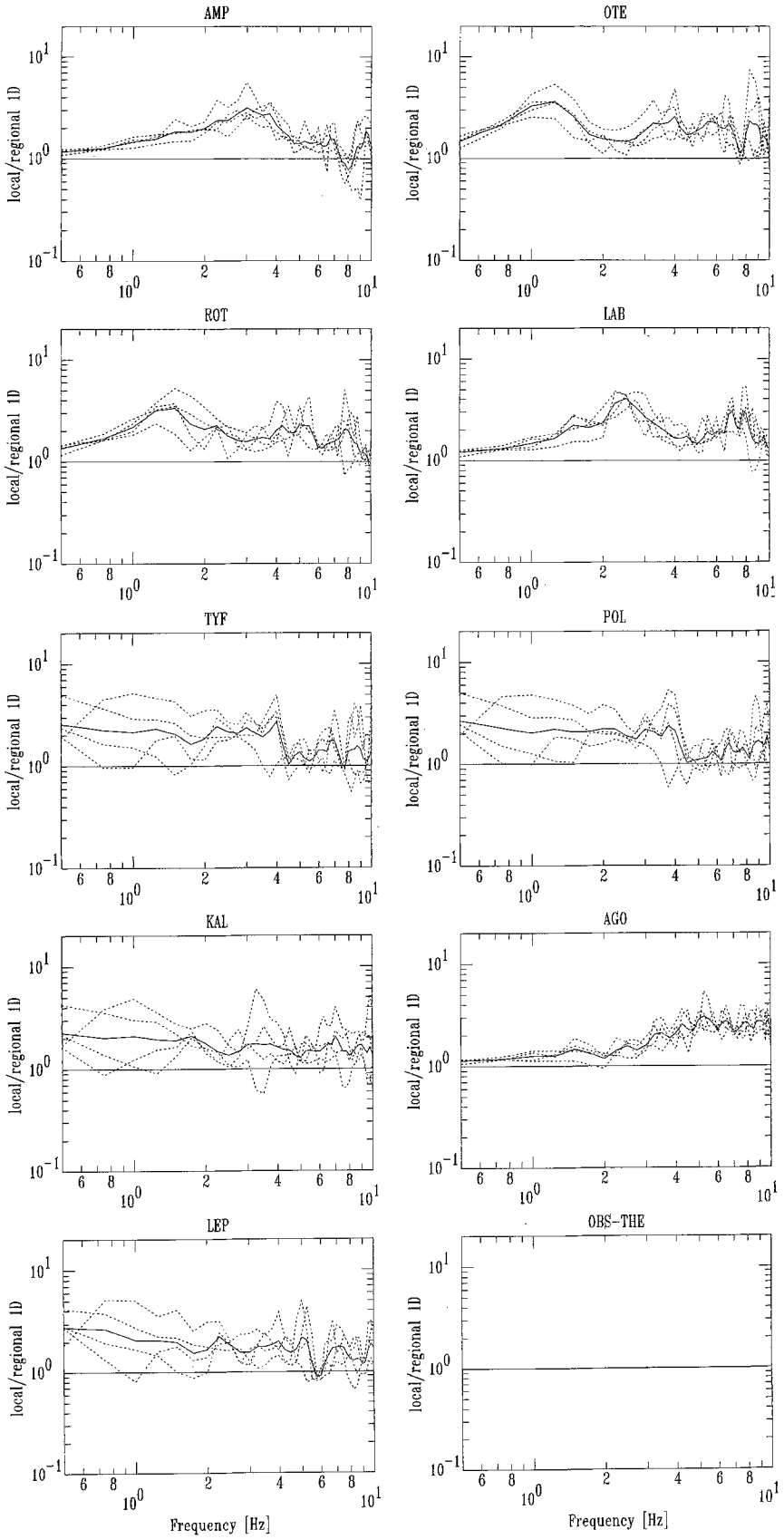


Figure 10. Local over regional 1D-model spectral ratios at each station for the radial components of the four events (dotted lines). Solid line represents the mean of all four ratios.

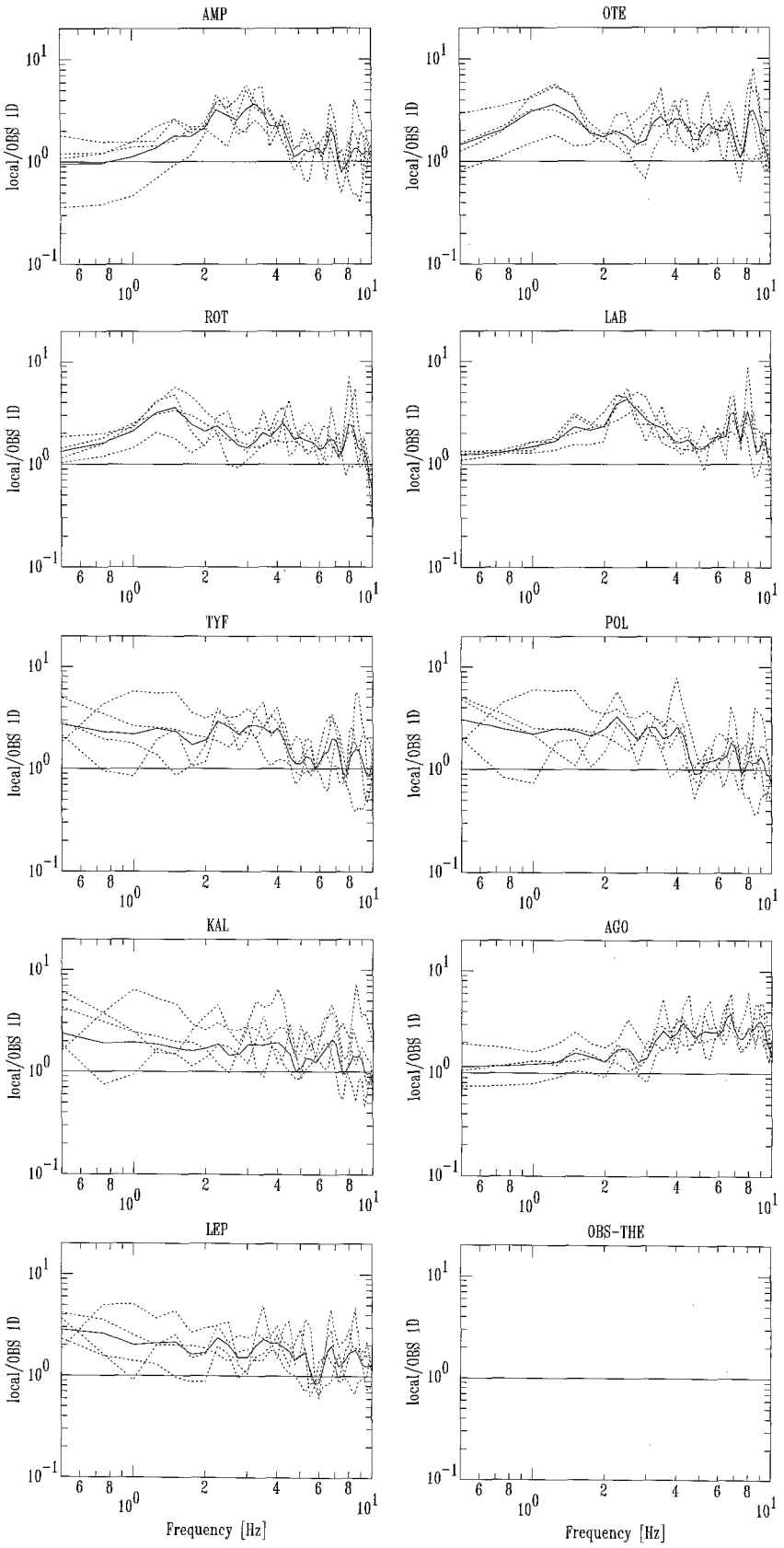


Figure 11. Variation of the local-to-reference station (OBS) spectral ratios for the radial components of the far and the corrected local events (dotted lines). Solid line represents the mean of all four ratios.

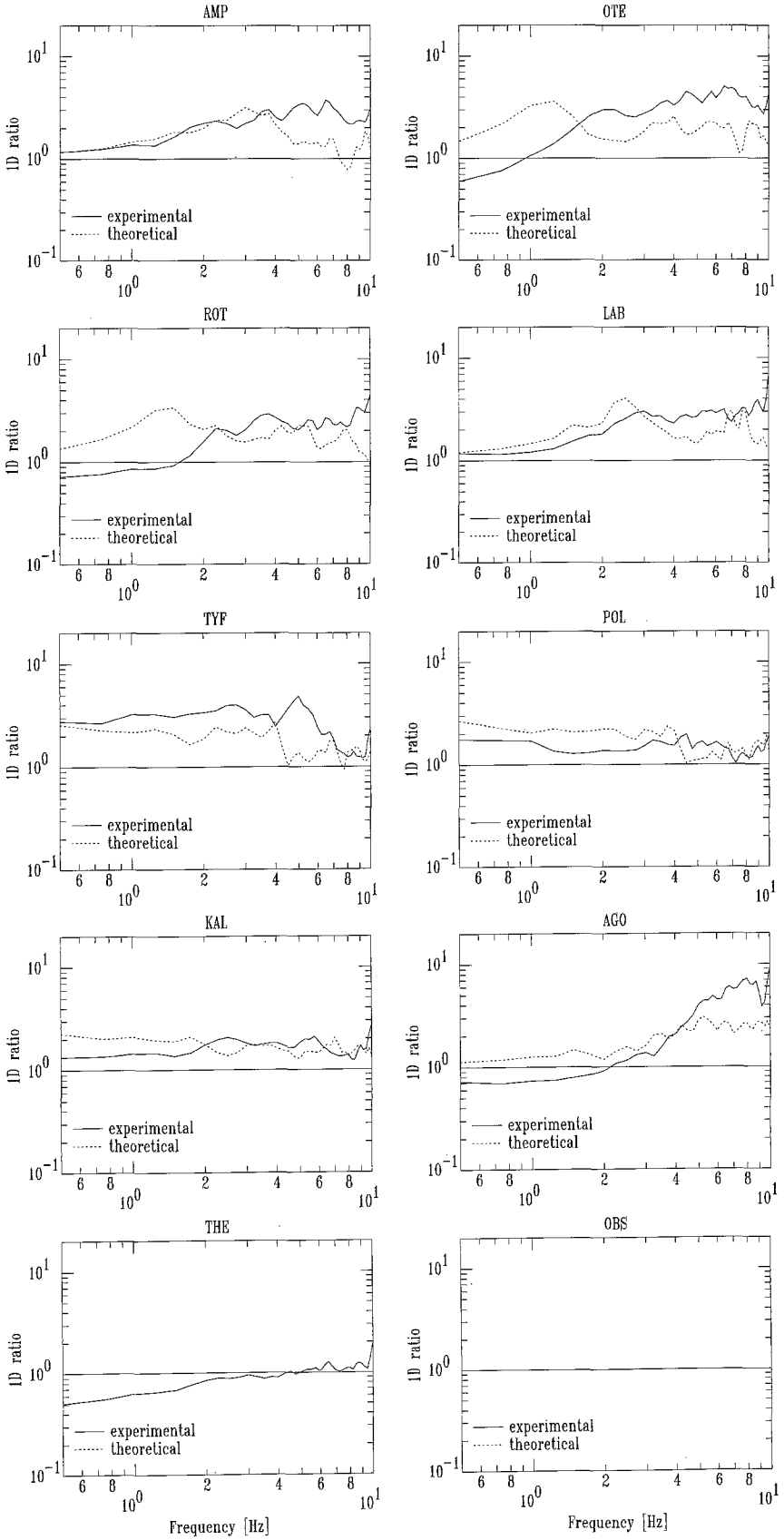


Figure 12. Comparison between the mean of spectral ratios of theoretical local-to-regional 1D model for the radial component (dotted line) with the mean of the SSR method derived from the experimental data (solid line).

In the SSR technique, this elimination is only hypothetical and is not always correct, because the spectral ratio applies to recordings at different sites. This result is in agreement with the observation of a relatively low standard deviation and good stability of the HVSR spectral ratio of a selected set of Greek strong-motion data (Theodulidis and Bard, 1995).

3. Regarding the obtained relations (valid for Thessaloniki) that connect the intensity increments $\delta I$ to the logarithm of the mean amplification at a site as obtained by the application of the SSR, we conclude that, given an estimate of the amplification at a site, it is possible to roughly predict the intensity increment at this site relatively to the intensity at a nearby rock site. However, one has to use the regression curve based on the frequency band most appropriate for the resonant frequency of the investigated construction at a given site. The possibility of estimating the expected macroseismic results at a given site can be very useful for future vulnerability studies, seismic hazard assessment, and seismic microzonation studies in urban areas.

The results obtained from the theoretical approach are as follows:

1. Estimates based on 1D anelastic models of the local structure under a given site permit one to obtain estimates of local site amplifications that are in general agreement with those derived from experimental techniques, in cases of regions with an approximately local 1D geology. This means it is possible to roughly estimate the amplifications at a site only on the basis of geotechnical and geological surveys. This is particularly useful in low seismicity areas.
2. In these approaches, the radiation pattern should always be taken into account because it can give unreliable results in case of radiation minima when the reference station technique is used and the event is close to the stations.
3. For events with equivalent source spectra and source–receiver distances much larger than the interstation distances, the energy of motion at low frequencies dominates and the estimated amplification in the low-frequency range, which depends on the geometry of the deeper part of the model, are better determined. On the contrary, for events of similar magnitude with short source–receiver distances, the energy is essentially at high frequencies and the amplification estimates depend more on the geometry and the characteristics of the superficial layers.

## Acknowledgments

We would like to thank D. Hatzfeld for organizing the experiment and all the people who helped in maintaining the stations in the city of Thessaloniki. We are grateful to G. Leventakis, who provided us the unpublished observations of the damages in Thessaloniki from the earthquake of 20 June 1978. F. Marrara helped a great deal with the theoretical 1D computations. This work was completed when the first author was as "free mover" at DST-Trieste in the ERASMUS-SOCRATES framework. Financial support was provided by the EC Project "EUROSEISMOD" (ENV4-CT96-0255), UNESCO-IGCP Project 414, and for the experimental part by DPPR/DRM, Contract Number 106/92. This work was also partially supported by the Regional Operational Program of the Region of Central Macedonia, Greece, SAE/2 046/2, 1998–2000.

## References

Aki, K. (1988). Local site effects on strong ground motion, in *Earthquake Engineering and Soil Dynamics II—Recent Advances in Ground Motion Evaluation,* 27–30 June, Park City, Utah.

Aki, K. (1993). Local site effects on weak and strong ground motion, *Tectonophysics* **218,** 93–111.

Anastasiadis, A. (1994). Contribution to the determination of the dynamic properties of natural greek soils, *Ph.D. Thesis* (in Greek), Department of Civil Engineering, Aristotle Univ. of Thessaloniki.

Bard, P. Y. (1992). Site-Effects: Basic physical phenomena and estimation methods for microzonation studies. Regional and International Training Course 1992 on Seismology and Seismic Hazard Assessment, Lecture and Exercise Notes, VII, 534–608, Interner Bericht, GeoForschungsZentrum Potsdam.

Bard, P. Y. (1995). Effects of surface-geology on ground motion: recent results and remaining issues, *Proceedings of 10th ECEE,* Duma (Editor), Balkma, Rotterdam, 305–323.

Bard, P. Y. and F. J. Chávez-García (1993). On the decoupling of surficial sediments from surrounding geology at Mexico City, *Bull. Seism. Soc. Am.* **83,** 1979–1991.

Boore, D. (1972). A note on the effect of simple topography on seismic SH waves, *Bull. Seism. Soc. Am.* **62,** 275–284.

Boore, D. (1973). The effect of simple topography on seismic waves: implications for the accelerations recorded at Pacoima dam, San Fernando Valley, California, *Bull. Seism. Soc. Am.* **63,** 1603–1609.

Borcherdt, R. D. (1970). Effects of local geology on ground motion near San Francisco Bay, *Bull. Seism. Soc. Am.* **60,** 29–61.

Borcherdt, R. D. and J. F. Gibbs (1976). Effects of local geological conditions in the San Francisco bay region on ground motions and the intensities of the 1906 earthquake, *Bull. Seism. Soc. Am.* **66,** 467–500.

Borcherdt, R. D., G. Glassmoyer, A. Der Kiureghian, and E. Cranswick (1989). Results and data from seismologic and geologic studies following earthquakes of December 7, 1988 near Spitak, Armenia, S.S.R., *U.S. Geol. Surv. Open-File Rept. 89-163A.*

Campillo, M., J. C. Gariel, K. Aki, and F. J. Sánchez-Sesma (1989). Destructive strong ground motion in Mexico City: source, path, and site effects during great 1985 Michoacán earthquake, *Bull. Seism. Soc. Am.* **79,** 1718–1735.

Carver, D. and G. Bollinger (1981). Aftershock of the June 20, 1978 Greece earthquake: a multimode faulting sequence, *Tectonophysics* **73,** 343–363.

Chávez-García, F. J. (1991). Diffraction et amplification des ondes sismiques dans le bassin de Mexico, *Ph.D. Thesis,* Universite Joseph Fourier de Grenoble, 331 pp.

Chávez-García, F., G. Pedotti, D. Hatzfeld, and P. Y. Bard (1990). An experimental study of site effects near Thessaloniki (northern Greece), *Bull. Seism. Soc. Am.* **80,** 784–806.

EERI (1994). Northridge earthquake, Preliminary Reconnaissance Report, Earthquake Engineering Research Institute, Oakland, California.

EERI (1995). The Hyogo-Ken Nanbu earthquake, Preliminary Reconnaissance Report, Earthquake Engineering Research Institute, Oakland, California.

Fäh, D. (1992). A hybrid technique for the estimation of strong ground motion in sedimentary basins, *Ph.D. Thesis,* Nr 9767, Swiss Federal Institute of Technology, Zurich.

Field, E. H. and K. Jacob (1995). A comparison and test of various site response estimation techniques, including three that are non reference-site dependent, *Bull. Seism. Soc. Am.* **85,** 1127–1143.

Field, E. H., P. A. Johnson, I. A. Beresnev, and Y. Zeng (1997). Nonlinear ground-motion amplification by sediments during the 1994 Northridge earthquake, *Nature* **390,** 599–602.

Finn, W. D. L. (1991). Geotechnical engineering aspects of seismic microzonation, *Proc. of the 4th International Conference on Seismic Zonation,* August 25–29, Stanford, California, vol. 1, 199–250.

Finn, W. D. L. and A. M. Nichols (1988). Seismic response of long period sites: lessons from the September 19, 1985 Mexican earthquake, *Canadian Geotechnical J.* Feb., 128–137.

Hatzfeld, D., V. Karakostas, G. Selvaggi, S. Leborgne, C. Berge, R. Guiguet, A. Paul, P. Voidomatis, D. Diagourtas, I. Kassaras, I. Koutsikos, K. Makropoulos, R. Azzara, M. Di Bona, Bacceeschi, P. Bernard, and C. Papaioannou (1997). The Kozani-Grevena (Greece) earthquake of 13 May 1995 revisited from a detailed seismological study, *Bull. Seism. Soc. Am.* **87,** 463–473.

Hough, S. E., R. D. Borcherdt, P. A. Friberg, R. Busby, E. Field, and K. H. Jacob (1990). The role of sediment-induced amplification in the collapse of the Nimitz freeway during the October 17, 1989 Loma Prieta earthquake, *Nature* **344,** 853–855.

Kudo, K. (1995). Practical estimates of site response—state-of-art report, 5th Conf. on Seismic Zonation, Vol. III, Nice, France.

Lachet, C. and P. Y. Bard (1994). Numerical and theoretical investigations on the possibilities and limitations of the Nakamura's technique, *J. Phys. Earth* **42,** 377–397.

Lachet, C., D. Hatzfeld, P. Y. Bard, N. Theodulidis, C. Papaioannou, and A. Savvaidis (1996). Site effects in the city of Thessaloniki (Greece). Comparison of different approaches, *Bull. Seism. Soc. Am.* **86,** 1692–1703.

Langston, C. A. (1979). Structure under mount Rainier, Washington, inferred from teleseismic body waves, *J. Geophys. Res.* **84,** no. B9, 4749–4762.

Lawson, A. C. (1908). The California earthquake of April 18, 1906: Report of the State earthquake investigation commission, Carnegie Institute, Washington, Publ. 87.

Lermo, J. and F. G. Chávez-García (1993). Site effect evaluation using spectral ratios with only one station, *Bull. Seism. Soc. Am.* **83,** 1574–1594.

Lermo, J. and F. J. Chávez-García (1994). Are microtremors useful in site response evaluation? *Bull. Seism. Soc. Am.* **83,** 1350–1364.

Ligdas, C. N. and J. M. Lees (1993). Seismic velocity constraints in the Thessaloniki and Chalkidiki areas (northern Greece) from a 3D tomographic study, *Tectonophysics* **228,** 97–121.

Nakamura, Y. (1989). A method for dynamic characteristics estimation of subsurface using microtremor on the ground surface, *QR Railway Tech. Res. Inst.* **30,** no. 1, 25–33.

Nogoshi, M. and T. Igarashi (1970). On the propagation characteristics of microtremor, *J. Seism. Soc. Japan* **23,** 264–280 (in Japanese with English abstract).

Nogoshi, M. and T. Igarashi (1971). On the amplitude characteristics of microtremor (part 2), *J. Seism. Soc. Japan* **24,** 26–40 (in Japanese with English abstract).

Panza, G. F. (1985). Synthetic seismograms: the Rayleigh waves modal summation, *J. Geophys.* **58,** 125–145.

Panza, G. F. and P. Suhadolc (1987). Complete strong motion synthetics, in *Seismic Strong Motion Synthetics,* B. A. Bolt (Editor), Academic, Orlando, Computational Techniques 4, 153–204.

Papazachos, C. B. (1998). Crustal P- and S-velocity structure of the Serbomacedonian massif (Northern Greece) obtained by non-linear inversion of travel times, *Geophys. J. Int.* **134,** 25–39.

Papazachos, C. B. and A. A. Kiratzi (1996). A detailed study of the active crustal deformation in the Aegean and surrounding area, *Tectonophysics* **253,** 129–153.

Papazachos, B. and C. Papazachou (1997). The earthquakes of Greece, *Editions Ziti,* 304 pp.

Papazachos, B. C., A. Mountrakis, A. Psilovikos, and G. Leventakis (1979). Surface fault traces and fault plane solutions of the May–June 1978 major shocks in the Thessaloniki area, Greece, *Tectonophysics* **53,** 171–183.

Pitilakis, K., A. Anastasiadis, and D. Raptakis (1992). Field and laboratory determination of dynamic properties of natural soil deposits, *Proc. 10th World Conference of Earthquake Engineering,* Madrid, Spain, 1275–1280.

Raptakis, D. (1995). Contribution to the determination of the geometry and the dynamic properties of soil formations and their seismic response, *Ph.D. Thesis* (in Greek), Department of Civil Engineering, Aristotle Univ. of Thessaloniki.

Raptakis, D., K. Pitilakis, and K. Lontzetidis (1993). Seismic methods in the evaluation of dynamic properties of soil formations, (in Greek), *Proc. 2nd Conf. of Hellenique Geophysical Union,* Florina, 5–7 May 1993, vol. 3, 349–359.

Raptakis, D., A. Anastasiadis, K. Pitilakis, and K. Lontzetidis (1994a). Shear wave velocities and damping of Greek natural soils, *Proc. 10th ECEE,* Wien 1994, vol. 1, 477–482.

Raptakis, D., E. Karaolani, K. Pitilakis, and N. Theodulidis (1994b). Horizontal to vertical spectral ratio and geological conditions: the case of a downhole array in Thessaloniki (Greece), E.S.C. XXIV Gen. Ass., Athens.

Raptakis, D., N. Theodulidis, and K. Pitilakis (1998). Standard spectral ratio and horizontal to vertical ratio techniques: data analysis of the Euroseistest strong motion array in Volvi-Thessaloniki (Greece), *Earthquake Spectra* **14,** 203–224.

Riepl, J. (1997). Effects de site: evaluation experimentale et modelisations multidimensionelles: application au site test EUROSEISTEST (Greece), *Ph.D. Thesis,* University of Joseph Fourier, Grenoble.

Riepl, J., P. Y. Bard, D. Hatzfeld, C. Papaioannou, and S. Nechtschein (1998). Detailed evaluation of site response estimation methods across and along the sedimentary valley of Volvi (EUROSEISTEST), *Bull. Seism. Soc. Am.* **88,** 488–502.

Silva, W. J. (1989). Site geometry and global characteristics, state of the art report, *Proc. of Workshop on Dynamic Soil Properties and Site Characterization,* National Science Foundation and Electric Power Research Institute, Palo Alto, California, November.

Singh, S. K., E. Mena, and R. Castro (1988). Some aspects of source characteristics of the 19 September 1985 Michoacan earthquake and ground motion amplification in and near Mexico City from strong motion data, *Bull. Seism. Soc. Am.* **78,** 451–477.

Steidl, J. H., A. G. Tumarkin, and R. J. Archuleta (1996). What is a reference site? *Bull. Seism. Soc. Am.* **86,** 1733–1748.

Soufleris, C., J. A. Jackson, G. C. P. King, C. P. Spencer, and C. H. Scholz (1982). The 1978 earthquake sequence near Thessaloniki (northern Greece), *Geophys. J. R. Astr. Soc.* **68,** 429–458.

Theodulidis, N. and P. Y. Bard (1995). Horizontal to vertical spectral ratio and geological conditions: an analysis of strong motion data from Greece and Taiwan (SMART-1), *Soil Dyn. Earthquake Eng.* **14,** 177–197.

Theodulidis, N., R. J. Archuleta, P. Y. Bard, and M. Bouchon (1996). Horizontal to vertical spectral ratio and geological conditions: the case of Garner Valley downhole array in southern California, *Bull. Seism. Soc. Am.* **86,** 306–319.

Geophysical Laboratory
Aristotle University of Thessaloniki
P.O. Box 352-1
GR-54006
Thessaloniki, Greece
(P. T., trian@lemnos.geo.auth.gr; P. M. H., takis@lemnos.geo.auth.gr)

Institute of Engineering Seismology and Earthquake Engineering (ITSAK)
P.O. Box 53
GR-55102 Thessaloniki, Greece
(N. T., ntheo@itsak.gr; C. P., costas@quake.itsak.gr)

Univerità di Trieste
Dip. di Scienze della Terra
Via Weiss 1
I-34127 Trieste, Italy
(P. S., suhadolc@geosun0.univ.trieste.it)

Laboratory of Soil Mechanics & Foundation Engineering
Aristotle University of Thessaloniki
GR-54006 Thessaloniki, Greece
(K. L., kostas@evripos.civil.auth.gr;
D. R., raptakis@evripos.civil.auth.gr)

Manuscript received 23 April 1998.